# PREDICTION OF MILL STRUCTURE BEHAVIOUR IN A TUMBLING MILL

Pär Jonsén [1], Bertil I. Pålsson [2], Kent Tano [3], Andreas Berggren [4]

[1] Division of Solid Mechanics, Luleå University of Technology, SE-97187 Luleå, Sweden,

[2] Division of Mineral Processing, Luleå University of Technology, SE-97187 Luleå, Sweden,

[3] Technology and Business Development, LKAB, SE-98381 Malmberget, Sweden,

[4] Technology and Development, Boliden Minerals, SE-93681 Boliden, Sweden

ABSTRACT

Computational demands and the lack of detailed experimental verification have limited the value of Distinct Element Method (DEM) modelling approaches in mill simulation studies. This paper presents the results of a study in which the deflection of a lifter bar in a pilot ball mill is measured by an embedded strain gauge sensor and compared to deflections predicted from finite element (FE) simulations. The flexible rubber lifter and the lining in a tumbling mill are modelled with the finite element method (FEM) and the grinding medium modelled with DEM. The deflection profile obtained from DEM-FE simulation shows a reasonably good correspondence to pilot mill measurements. To study the charge impact on the mill structure two different charges are used in the simulations. The approach presented here is a contribution to the validation of DEM-FE simulations and an introduction to the description of a bendable rubber lifter implemented in a DEM-FEM mill model. It opens up the possibility to predict contact forces for varying mill dimensions and liner combinations. FEM is especially valuable in this case, since there are readily available libraries with material models. This is a follow-up work to previous preliminary result from a mono-size ball charge interaction study.

## 1 Introduction

Autogenous (AG) and semi-autogenous (SAG) mills often operate in a metastable state because of the difficulty to balance the rate of replenishment of large ore particles from the feed with the consumption in the charge. This has led to an increased interest in obtaining an accurate and direct measurement of

mill load and the behaviour of the mill charge. Several parameters do significantly influence the effectiveness of the grinding operation; however, some of these parameters are either difficult or laborious to measure. Intermittent in-situ measurements of these are most often prone to errors and there is often a long time-delay before the acquired data is fed to the control system. Also, an understanding of the charge motion within the mill is of importance in mill optimisation. Both the breakage of ore particles and the wear of liners/ball media are closely linked to the charge motion. To study these phenomena in a physically correct manner, suitable numerical models for the different parts of the mill system has to be utilised.

For a long time distinct element methods (DEM) has been used as simulation tools to gain insight into particulate flow processes. When applied to grinding it gives an opportunity to study several aspects of grinding in greater detail than has been possible to date, e.g. charge viscosity and charge size distribution. DEM might be used to describe and visualise the motion of the grinding charge and how it is influenced by both design and operating parameters. Furthermore, DEM calculations provide useful estimates on collision forces, energy loss spectra and power consumption. DEM was introduced by Cundall (1971) for analyses of rock-mechanic problems. Today, DEM is an important tool for analyses of particle systems. An initial attempt to use DEM to describe the interaction of large grinding balls, and the lining was presented by Rajamani (2000). However, some improvements of today's DEM models can be identified, for example the structure of the mill (geometry and material composition) may be modelled with FEM.

For structural analysis the finite element method (FEM) is the most developed and used numerical method. FEM is a numerical solution method based on continuum mechanics modelling, a constitutive relation for the actual material is described and the governing equations are solved. A variety of different constitutive models for a large number of materials are implemented in a modern finite element (FE) code.

The comminution process is complex and to include all phenomena that occur in a single numerical model is today not possible. Therefore, modelling the physical interaction between the charge and the mill structure is the major goal in this work. Here, the contact between particles modelled with DEM and the structure modelled with FEM is the major key in the model. The DEM-FEM model can predict the classical DEM results, but can also predict responses from the mill structure like, e.g., stress and strain. All parts of the mill system will affect its response and a DEM-FEM model gives the opportunity study the influence of the mill structure. The validation of this task is done by comparing numerical results with experimental measurements from pilot grinding with an instrumented rubber lifter. This work is a continuation of previous preliminary work on DEM-FEM modelling of tumbling milling processes, see Jonsén (2009).

## 2 Experimental setup

A simplified view of the sensor is shown in Figure 1, Tano (2005). The mill has several lifters one of them (marked 1) is equipped with a leaf spring whose deflection is measured by the strain gauge (marked 2). As the mill rotates and the lifter with the sensor dips into the charge, the force acting on the lifter increases, which in turn, causes a deflection. The strain gauge mounted on the leaf spring converts this deflection to an electric signal. The signal is then amplified, filtered and transmitted to a computer. The sensor system is marketed by Metso Minerals under the name Continuous Charge Measurement system (CCM), see Dupont (2001).

A typical deflection profile of the sensor signal and an attempt to divide it into different segments is shown in Figure 2. The boundaries and size of the partitions are determined by engineering knowledge of the grinding process. Each segment in Figure 2 illustrates an important dynamic event during the passage of the sensor-equipped lifter bar under the mill charge. The ordinate in Figure 2 shows the deflection of the lifter bar, which indirectly corresponds to the force acting on it and the abscissa is the mill rotation angle with a resolution of 1°.
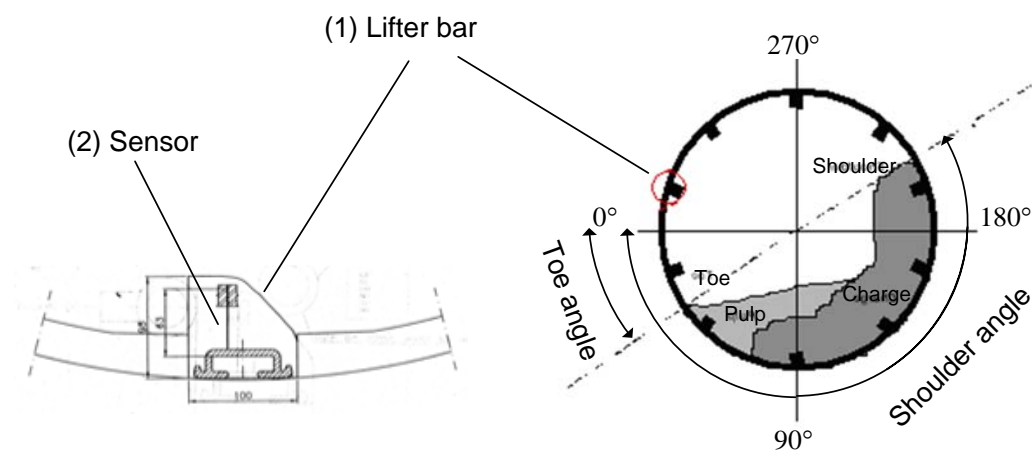


Figure 1. To the right a cross section of a mill with a horizontal reference line, the left part shows the lifter bar (1) with a strain gauge sensor embedded (2), from Tano (2005).

The sensor signature reflects different charge features such as mill volume, position and behaviour of the mill charge. Both toe region (S2) and shoulder region (S6) are well known, and can be used to calculate the volumetric mill load and the angle of repose. Collectively, these data give a good measure of the location of the charge. The other segments are less known but are expected to provide information about grinding efficiency. Such features can be extracted from the sensor signal for the purpose of process monitoring and diagnosis of process performance.
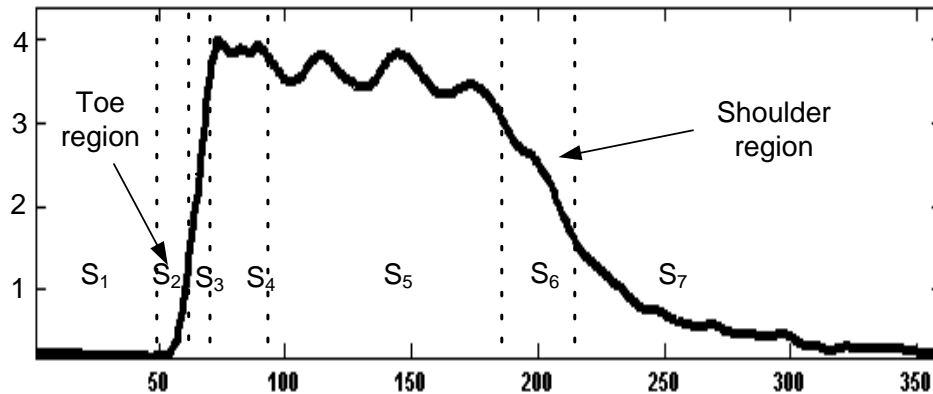
Figure 2. Segmentation of a typical sensor signal during its passage in the charge Tano (2005).

Table 1. Sensor lifter bar signal segmentation and grinding load features Tano (2005).

| Segment | Lifter bar angle | Process feature |
|---|---|---|
| $S_1$: the sensor lifter bar (SL) is still in the air | < 50° | |
| $S_2$: the SL hits the ball charge and starts to get submerged in the charge | 50°- 70° | Indicate the toe position of the charge, and if present, the slurry pool |
| $S_3$: the SL starts to bend forward due to turbulence in the toe area | 70°- 85° | Rate of charge varies with mill speed |
| $S_4$: the SL is at peak bending | 75°- 90° | Both speed and charge level has an influence, wear of lifter |
| $S_5$: the SL is moving through the charge | 80°- 190° | Indication of every lifter bar hitting the charge |
| $S_6$: the SL has gradually decrease the bending and is at take-off position | 190°- 215° | Indicates the shoulder position of the charge |
| $S_7$: the SL is leaving the ball charge and starts slowly to rise to an upright position | > 215° | |

Table 1 provides a summary of the stages during one mill revolution. The lifter bar angles given in Table 1 correspond to the positions marked in Figure 2, as a reference in these measurements is the horizontal line, which corresponds to 0 degrees at the 9 o'clock position. In this work, an attempt is made to identify the corresponding segments in a predicted deflection profile obtained from DEM simulation. The toe/shoulder position in particular will be compared for validation purposes.

## 2.1 Experimental conditions

The pilot mill is 1.414 m in diameter and 1.22 m in length. It is a grate-discharge mill, equipped with 12 rubber lifters of square size 0.1 m and a face angle of 45 degrees. Steel balls with a diameter ranging between 10-30 mm and a density of 7800 kg/m$^3$ were used in the experiments. The test material, a hematite pellet feed with d50 around 35µm and a solids density of 5200 kg/m$^3$, was chosen to get stable grinding conditions with respect to feed size variations. Feed rate was kept constant at approx. 1.5 tonne/h. Four experiments were run with the mill speed at 73% and 78% of critical speed ($n_c$) for two levels of mill filling (J = 25% and 35% by volume). The embedded strain gauge sensor measured the load position (toe and shoulder) using the CCM algorithm, proprietary of Metso Minerals.

## 3  Modelling

The model of the mill is a combined model consisting of a charge modelled with DEM and the mill structure modelled with FEM. The mill structure consists of rubber lifter and liners made of rubber and a mantel made of solid steel. Here the rubber is modelled as a hyper-elastic material and the mill mantel is modelled as a rigid material. The ball charge is modelled with DEM.

### 3.1  Mill structure model

The original length of the mill is 1.22 m, however, in the model only a slice of 0.10 m is modelled. The structure consisting of rubber liners, rubber lifters and a solid mantel are modelled with eight node solid elements. This type of element is fully integrated with a reduced integration of the pressure part to avoid volumetric locking of the element. For the elastic behaviour of the rubber a Blatz-Ko hyper-elastic model is used (Blatz and Ko 1962). A classic approach to model rubber material is to use a hyper-elastic model. A hyper-elastic material is an ideally elastic material for which the stress-strain relationship derives from a strain energy density function. Experimental data for the rubber was provided by the supplier of the lining.
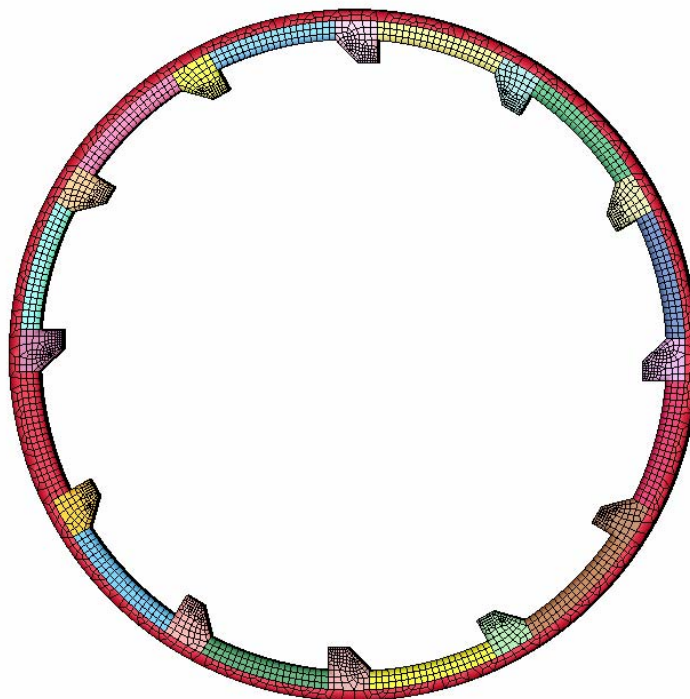


Figure 3. FEM model of the mill containing lifter and liners in rubber and a solid mantel modelled with rigid material.

In Figure 3, the FEM model of the mill is shown. The mill model contains 25 parts, 12 lifters and liners and a solid mantel. The force response on the rubber structure is an interesting characteristic of the mill system. Contact force history of one of the lifters during a number of evolutions is studied in detail. To study

forces in the liners a section plane is added in the liner behind the studied lifter between elements in row three and four. The action of the section plane is to add all forces in the plane together. In Figure 4, a detailed illustration of the lifter mesh with the added section plane is shown. A total number of 9401 solid elements are used to model the structure. The deflection of the lifter was tracked by monitoring the positions of two nodes at the locations nearest the true base and tip of the lifter, see Figure 4. The friction coefficients of the particle-particle contact was set to $\mu = 0.5$ and for the particle-wall contact to $\mu = 0.9$ based on values published by Rajamani (2000). For the contact between the particles and the structure a "nodes to surface" contact is used. This type of contact is a so called one way contact which works well when the master side is a rigid body. A viscous damping of 60% is used in this contact based on the particle-particle bouncing collision behaviour observed in the current calculations.
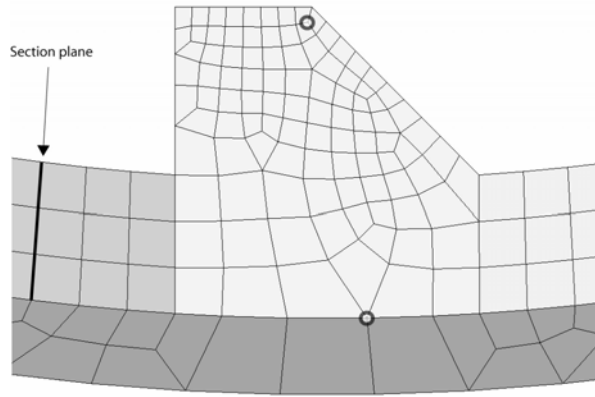


Figure 4. The mesh of the lifter with the section plane, also the locations of the nodes at the tip and base are shown.

## 3.2    Particle density

Because of the two-dimensional representation, the balls in the numerical mill are represented by rods rather than spheres. In this case, the disk thickness is set equal to the length of the pilot mill model, 0.1 meters. In order to mimic the mass and inertia of a string of charge balls rather than a solid rod, the density of the particles representing the charge was lowered accordingly. The consequence of this two-dimensional representation is that any single particle impacting the lifter within the two-dimensional model is actually simulating the simultaneous impact of a string of charge balls running the full length of the mill. Such simultaneous impact is not likely happening in reality and so this should be considered when interpreting deflection results from the 2D model.

## 4    Results

In the numerical study the mill fill was $J = 25\%$ and speed 73% of critical rotational speed. Two different ball charges are used in the study. One with a constant particle diameter of 20 mm and one with a particle diameter distribution from 15 to 25 mm, one third of each type, also called graded charge. In Figure 5

the two cases are shown at steady state. The graded charge tends, according to the simulation to have more voids in the packing pattern of the particles and the toe angle is smaller.
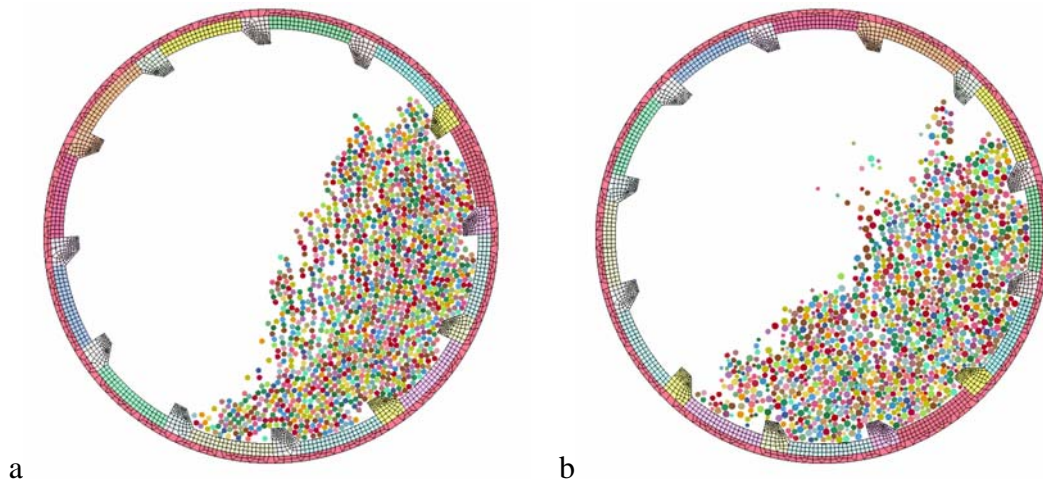


a                                                                b

Figure 5. In a. the non-graded charge with 20 mm diameter particles and in b. the graded charge with a diameter distribution of 15-25 mm.

## 4.1    DEM-FEM interaction

The rotation of the mill induces charge motion. During this motion particle-particle and particle-structure interactions occurs in the mill system. The contact between particles and structure of the mill results in a load to the structure of the mill that induces strain and stress into the structure. This load also induces mechanical waves in the whole structure. To study the charge impact on the mill structure during the milling process one can study forces and deflections of a lifter in the system. To observe the forces that go through the system of liners a section plane is introduced in the liner behind the studied lifter. The deflection of the lifter is also analysed and compared to the experimental measurements.
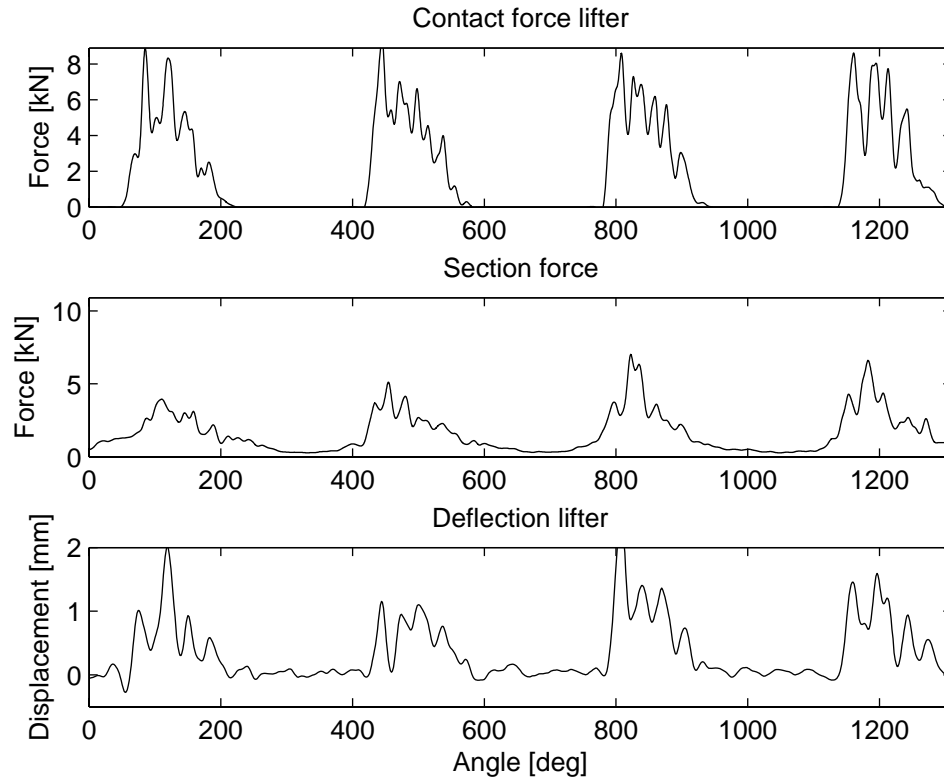
Figure 6. Results from the numerical analysis, (non-graded charge) a, contact force on a lifter in the system, b. forces in the section plane behind the lifter and c, deflection of the lifter.

As the model is just a small segment of the actual mill the forces are recalculated to a 1.22 m long mill. Results for contact forces, section forces and deflection for four passages for the non-graded and the graded charge are shown in Figure 6 and 7. In the beginning of the simulation, the system has a start-up procedure and the system has to find steady state. This explains why the first passage show a dissimilar response compared to the following three passages. During passage in the ball charge contact forces on the lifter have a maximum peak force of about 8.5 kN for the non-graded charge and 7.5 kN for the graded ball charge. For the non-graded charge the peak occurs around an angle of 80° and for the graded charge around 100°. The non-graded charge shows the highest peak in the beginning of the passage through the charge while the contact force pattern for the graded charge is more symmetric. Between the passages the force is zero. The section force shows a symmetric pattern for both cases and the peak are around 6.5 kN for both cases. Between the passages the section force shows a base noise level which suddenly increases as the lifter comes in contact with the ball charge.
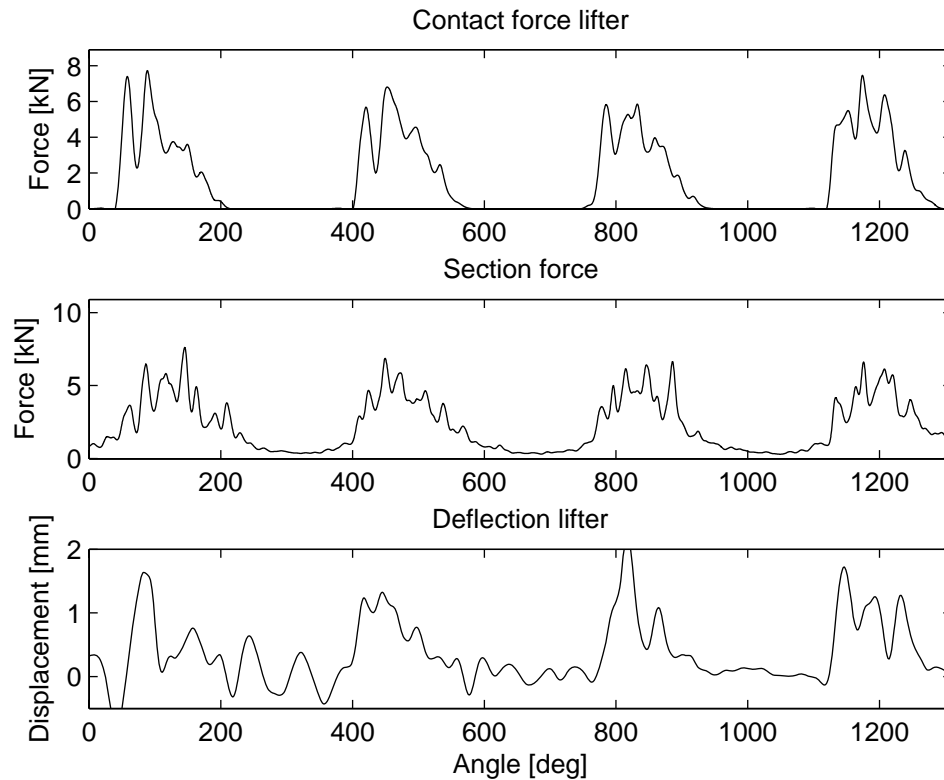
Figure 7. Results from the numerical analysis, (graded charge) a, contact force on a lifter in the system, b. forces in the section plane behind the lifter and c, deflection of the lifter.

For the non-graded charge the maximum displacement is 1.6 mm and found in the second peak. The maximum displacement for the lifter in the graded charge is about 1.7 mm and found in the first peak. Both cases appear to stabilise around 1 mm to decrease even more at the end of the passage. Comparing the deflection with the experimental results from Tano (2005) show an acceptable agreement.

A comparison of the response from the two load cases for the fourth passage is made. In Figure 8 the contact force signature for the two cases are shown. The behaviour is different in the two cases. The non-graded charge gives the largest maximum value and it is found in the first peak. The maximum value of the contact force for the graded charge is found in the second peak. Due to a higher toe angle the force starts to rise later for the non-graded charge than for the graded charge. The decrease of the force is similar for the two cases. For the fourth passage, the section forces are compared for the both cases, see Figure 9. In the case with the graded charge the section force seems to have more strong peaks compared to the case with a non-graded charge. The non-graded charge has a distinct maximum peak around 100°. Generally the section forces are smaller than the contact forces acting on the lifter.
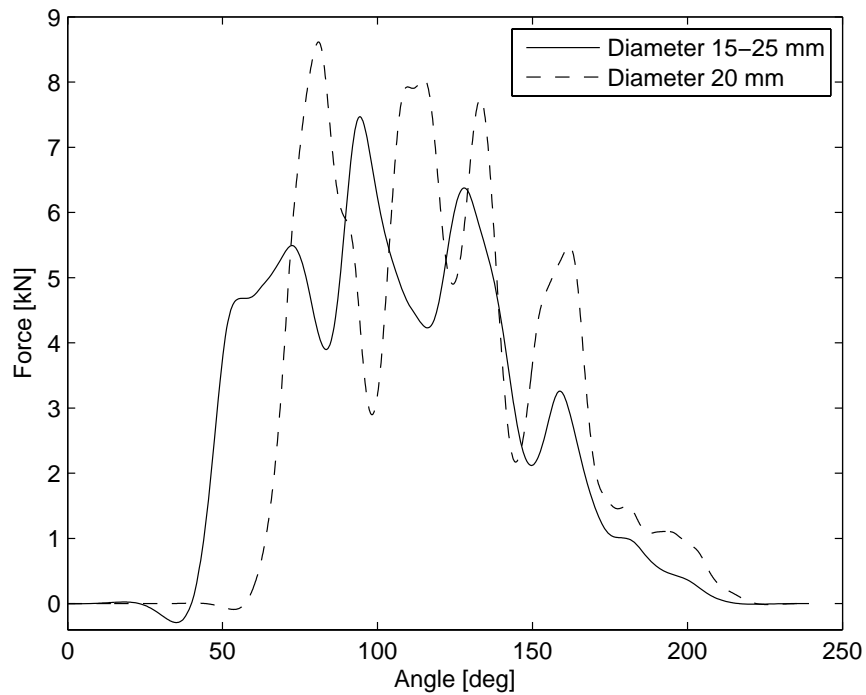
Figure 8. Contact force on the lifter during the fourth passage, solid line graded charge and dashed line non-graded charge.
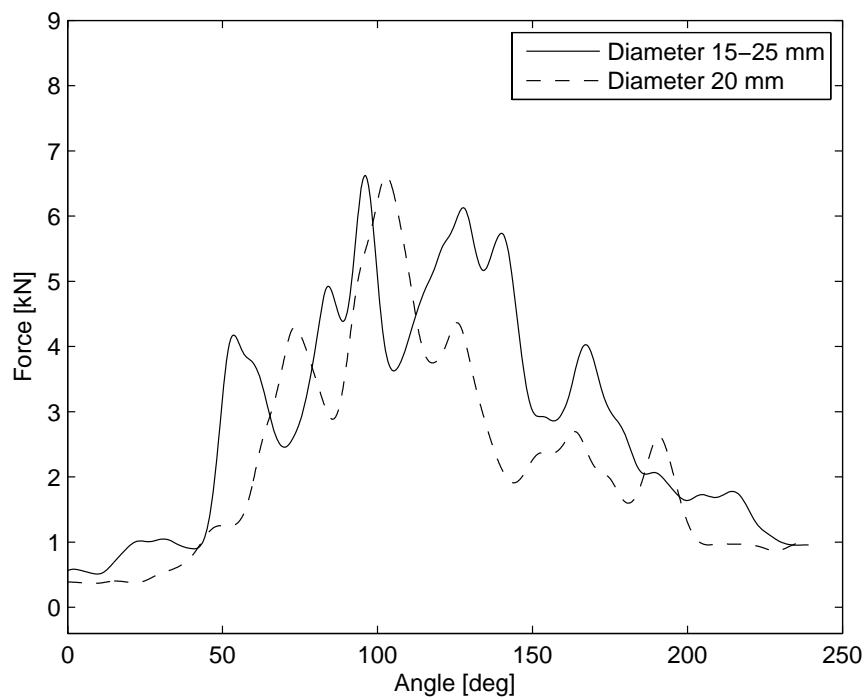


Figure 9. Section force on the lifter during the fourth passage, solid line graded charge and dashed line non-graded charge.

The displacement of the lifter during the fourth passage for the two cases is shown in Figure 10. Both cases have a similar signature but the maximum peak

for the graded charge occurs as the lifter submerges into the charge around 70°. Even though the first and the second peak are almost equally high for the non-graded charge the maximum value is found in the second peak around 115°. The toe angle is around 62° for the non-graded charge and around 48° for the graded charge. The shoulder angle for the non-graded charge is 235° and 220° for the graded charge. The peaks are slightly higher for the graded charge. The deflection profiles of the lifters have been compared and are in agreement with both calculated and measured result of Tano (2005).
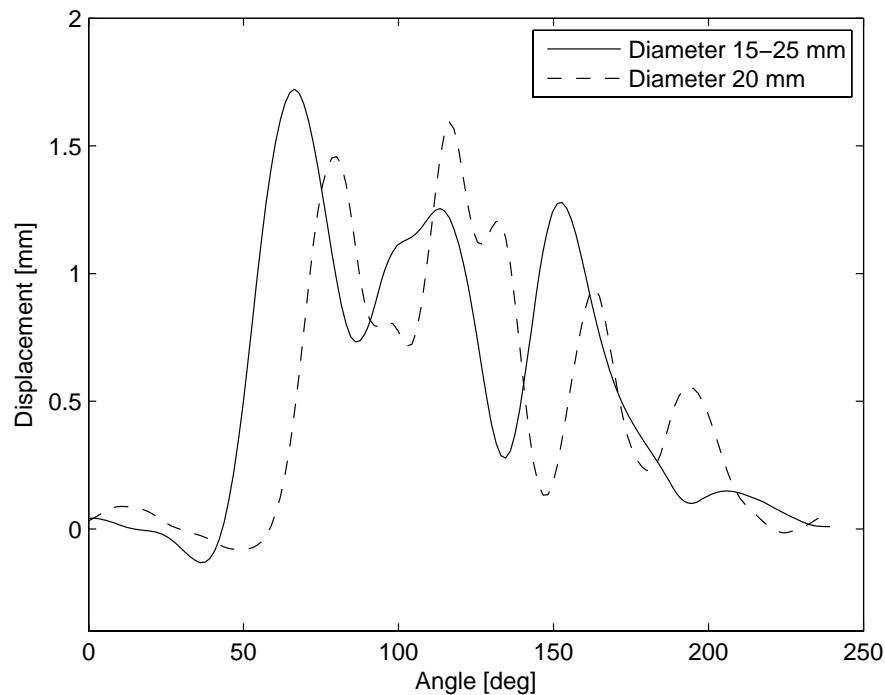


Figure 10. Displacement of the lifter during the fourth passage, solid line represents the response from the graded charge and dashed line the non-graded charge response.

The structure will respond to deformation upon the incoming load from the charge. These deformations will give rise to strains and stresses which are dependent on the material properties of the structure. A snapshoot of the von Mises' stress field for two lifters and the liner in between and during their passage in the charge is shown in Figure 11. This is one of the additional properties that are available from the FE-program.
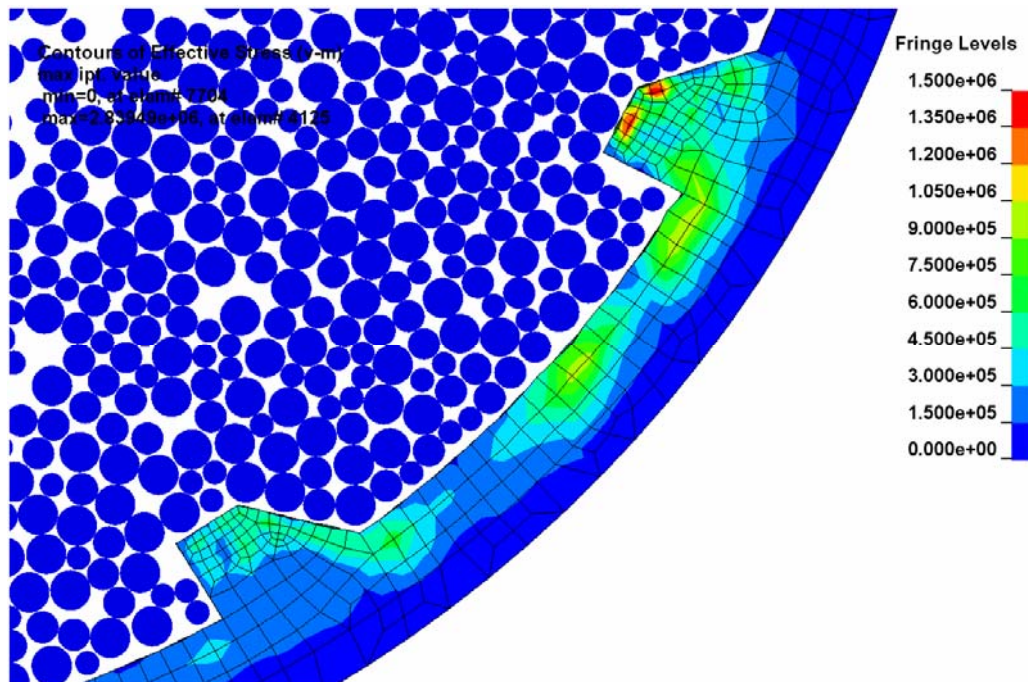
Figure 11. A snapshot of the von Mises' stress field for a part of the mill model during its passage through the charge.

## 5      Discussion and conclusion

DEM have been used in simulations of tumbling mill processes. A pure DEM model provides useful information on charge motion, collision forces, energy loss spectra and power consumption. This is important for improving the milling efficiency and gain more understanding of the process itself. For improved estimations of the complex nature of the milling process better and more physically precise models are desirable. Steps towards more physically correct numerical descriptions of mill systems are combined DEM-FEM models. With a DEM-FEM model structural response and its influence of the charge motion can be studied. The model gives the opportunity to optimize the material selection of the mill structure. Also, today's FE-codes give the opportunity to vary between materials and its mechanical response. Critical response values for e.g. stress and strain can be identified during the milling process. Forces and mechanical waves in the structure can be found.

Mechanical response of the mill structure is predicted by constitutive models included in the FE formulation. The DEM-FEM model predicts mechanical responses from the charge load on the whole mill. It may also, predict forces travelling in the lining, and by that the echoes from consecutive lifter-charge hits. This gives an opportunity to validate signals from on-shell sensor types.

Bending of the flexible rubber lifter and the corresponding stress field during its passage in the ball charge is shown in Figure 11. The major difference between DEM only and DEM-FEM models is that the latter give a direct coupling between force, stress and displacement for the whole mill system.
To include the mill structure response in the numerical models gives more information regarding charge motion and may result in better correlation

between experimental measurements and numerical models. The DEM-FEM model should also be a more physically correct model compared to a DEM model with rigid walls.

Lifter representation by FEM instead of DEM particles is more computationally effective. In the present case, all lifters and liners for the whole mill are modelled with the real material behaviour. This will give a physically more accurate presentation of the system. Also, the liner design has a large influence on the charge motion. A correct liner design may minimize energy consumption and increase the efficiency of the milling process. To be able to predict this motion will be of great value for designers of mill wear systems.

We can see a difference between the non-graded and graded charge, i.e. the toe and shoulder angels are different, contact forces behaviour are also dissimilar, the displacement of the rubber lifter is different etc. One obvious difference is the packing of the charges and according to that the charge sensitivity to both particle-particle and particle wall friction. This will result in different stiffness of the charge. The stiffness will also differ inside the charge. This study is left out side the scope of this work but will be addressed in future work.

In future work a better representation of the current model will be implemented together with a particle based model for the slurry.


## 6    Acknowledgement

## 7    References

Blatz, P.J., and Ko, W.L., 1962, Application of Finite Element Theory to the Deformation of rubber Materials, Trans. Soc. of Rheology, 6, 223-251.

Cundall P.A., 1971, A computer model for simulating progressive large scale movements in blocky rock systems. In: Proceedings of the symposium of the international society for rock mechanics, Nancy, France. Vol.1, paper no. II-8.

Dupont J.F., Vien A., 2001, Continuous SAG Volumetric Charge Measurement. In: Proc. 33rd Ann. Can. Min. Proc. AGM, CIM, Ottawa, pp.51 - 67.

Jonsén P., Alatalo J., Pålsson B. I., Tano K., 2009, Prediction of contact forces between a grinding charge and mill lifters. /. I: 12th European Symposium on Comminution and Classification ESCC 2009,

Rajamani, R.K., 2000, Semi-Autogenous Mill Optimization with DEM Simulation Software. In: Control 2000 – Mineral and Metallurgical Processing.

Society for Mining, Metallurgy, and Exploration, Inc., Littleton, CO., USA. pp. 209-215. ISBN 0-87335-197-5

Tano K., 2005, Continuous Monitoring of Mineral Processes with Special Focus on Tumbling Mills – A Multivariate Approach, Doctoral Thesis, 2005:05, Luleå University of Technology, Sweden.